THE JOURNAL OF PHYSICAL CHEMISTRY C

Subscriber access provided by NANJING UNIV

Article

Electrodeposition of Periodically Nanostructured Straight Cobalt Filament Arrays

Xiao-Ping Huang, Wei Han, Zi-Liang Shi, Di Wu, Mu Wang, Ru-Wen Peng, and Nai-Ben Ming

J. Phys. Chem. C, **2009**, 113 (5), 1694-1697 • Publication Date (Web): 13 January 2009

Downloaded from http://pubs.acs.org on February 2, 2009

More About This Article

Additional resources and features associated with this article are available within the HTML version:

- Supporting Information
- Access to high resolution figures
- Links to articles and content related to this article
- Copyright permission to reproduce figures and/or text from this article

View the Full Text HTML

ACS Publications
High quality. High impact.

The Journal of Physical Chemistry C is published by the American Chemical Society. 1155 Sixteenth Street N.W., Washington, DC 20036

Electrodeposition of Periodically Nanostructured Straight Cobalt Filament Arrays

Xiao-Ping Huang, Wei Han, Zi-Liang Shi, Di Wu, Mu Wang,* Ru-Wen Peng, and Nai-Ben Ming

National Laboratory of Solid State Microstructures and Department of Physics, Nanjing University, Nanjing 210093, China

Received: August 28, 2008; Revised Manuscript Received: November 28, 2008

Arrays of straight cobalt filaments with periodic corrugation on the surface are electrodeposited on a glass substrate without using templates. The corrugated structures on the filaments are induced by the spontaneous oscillation of electric voltage in electrodeposition, and the periodicity can be tuned by applying different electric currents. Magnetic force microscopy indicates that when the interfilament separation is large, the magnetic domains are regularly aligned on the filament. Each corrugated structure on the filament surface corresponds to a local single magnetic domain. The domains become random when the interfilament separation becomes very small. We suggest that our results could be helpful in understanding the formation of magnetic domain patterns on a microscopic scale and may have potential application in spintronics.

I. Introduction

In ferromagnetic materials, magnetic domains are spontaneously formed in order to decrease the demagnetization fields and thus minimize the magnetostatic energy. Formation of magnetic domains depends on the balance of exchange energy, magnetostatic energy, and anisotropy energy.[1] The principle is that the gain in magnetostatic energy due to the reduced demagnetization field should be larger than the energy cost for the domain wall formation. Because of the developments in photolithography technology and characterization methods, much effort has been devoted to study the domain structure in square dots,[2−5] disks,[6−11] and wires or stripes[12−15] on nanoscale in recent decades. By tuning the shape and the separation of the magnetic elements, one may modify the conformation of magnetic domains and hence optimize the magnetic property.[16] Most recently, domain structures have attracted even more attention due to the attempts to manipulate magnetic domain walls by pulses of spin-polarized electric current in order to develop a prospective racetrack memory device.[17,18] It is expected that the static and dynamic behaviors of domain walls on the nanowires will determine the properties of the device. For this purpose, formation of periodically ordered magnetic domain structures is the first important step. Conventionally the magnetic nanostructures used in spintronics studies are fabricated by the state-of-the-art electron-beam lithography or focused ion beam facility, which are normally costly and time-consuming. We have developed a different approach, known as ultrathin layer electrochemical deposition (ULECD),[19−21] to fabricate quasi-two-dimensional metallic filament arrays with periodic nanostructures bottom-up, with the periodicity varying from a few tens of nanometers to sub-micrometer. This method was initially developed for the fabrication of copper filaments, on which the periodic nanostructures correspond to the spontaneously alternating deposition of copper and cuprous oxide.[19−21] Yet this method is readily being applied for the deposition of other metals, including ferromagnetic metals.

In this paper, we report for the first time the electrochemical deposition of straight nanostructured cobalt filaments by ULECD. With magnetic force microscopy (MFM), we demonstrate that the pattern of magnetic domains on the filaments depends on the interfilament separation. For the widely separated filaments, the magnetic domains are well aligned, forming a queue of ordered domain structures along the filament. When the filaments are very closely positioned, the regularity among the domains vanishes. Computer simulation has been applied to simulate the magnetic domain patterns in order to understand the change of domain configuration when the interfilament separation is varied.

II. Experimental Methods

In a conventional electrodeposition system, various disturbances in front of the deposition interface, such as fluctuation of concentration field[22] and convection in fluid phase,[23−26] including electroconvection,[27−30] affect the deposition process significantly. Consequently, the morphology of the electrodeposits is usually ramified and fractal-like.[31,32] In order to suppress the noisy disturbances in electrodeposition, the ULECD method has been invented.[19,20] In ULECD, a Peltier element is placed underneath the electrodeposition cell in order to decrease temperature and to solidify the electrolyte. During the solidification process, part of the salt in electrolyte is expelled from the ice due to the partitioning effect.[33,34] When equilibrium is eventually reached at the selected temperature (−4 °C, for example), an ultrathin layer of concentrated electrolyte remains between the ice of electrolyte and the glass boundary of the electrodeposition cell, as marked by ⑥ in Figure 1. The thickness of this ultrathin layer depends on the temperature, the initial concentration of electrolyte, and the amount of electrolyte solution in the deposition cell. In our system the typical thickness of this layer is of the order of several hundreds of nanometers.[20] Details of the experimental setup can be found in our previous publications.[19−21] In the current experiment, $CoCl_2$ aqueous electrolyte is prepared by dissolving $CoCl_2$ (analytical pure, 99.0%) with deioned ultrapure water (Millipore, electric resistivity 18.2 MΩ·cm), and the concentration is 0.02 M. Parallel, straight electrodes are made of pure cobalt wire (99.995% pure, 0.1 mm in diameter, Alfa Aesar) and are sandwiched by two glass plates (substrates). The separation of the electrodes is 10

* To whom correspondence should be addressed, muwang@nju.edu.cn.

10.1021/jp807673h CCC: $40.75 © 2009 American Chemical Society
Published on Web 01/13/2009

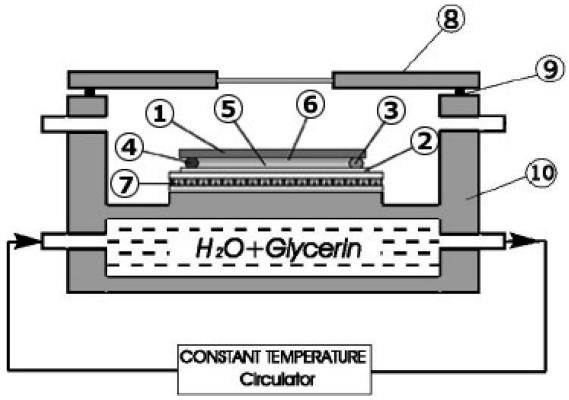

Figure 1. Schematic diagram of the experimental setup to generate the ultrathin electrolyte film and to electrodeposit the metallic filaments: (1) top glass plate; (2) bottom glass plate; (3) cathode; (4) anode; (5) ice of the electrolyte; (6) ultrathin electrolyte layer trapped between the ice of electrolyte and the glass plate; (7) Peltier element; (8) top cover of the thermostated chamber with glass window; (9) rubber O-ring for sealing; (10) thermostated chamber to keep the selected temperature for electrodeposition.

mm. The temperature of the electrodeposition cell is carefully decreased to −4 °C by a programmable thermostat (Polystat 12108-35, Cole-Parmer). In order to get a perfect crystalline ice of electrolyte, repeated solidification and melting is applied with the help of the Peltier element, until only one or just a few nuclei of ice remain in the deposition cell. The temperature decreasing rate is kept low in order to resume the flat interface in solidifying the electrolyte. Consequently a homogeneous, ultrathin layer of concentrated aqueous electrolyte of $CoCl_2$ is formed. Galvanostatic electrodeposition is used by applying a constant electric current in the range of 10−20 μA. In our system the unique phenomenon is that with galvanostatic (potenostatic) mode the voltage (current) across the electrodes may spontaneously oscillate.[19−21,35] The spontaneous oscillations result in the periodic structures on the electrodeposits. For cobalt electrodeposition, the cobalt filaments initiate from the cathode, nucleate on the glass substrate, and develop toward the anode. The cobalt filaments stick firmly on the glass substrate. The electrodeposits on the glass plate are rinsed with ultrapure water and dried in a vacuum chamber for further analyses.

The morphology of the cobalt electrodeposits is observed by scanning electron microscopy (LEO 1530VP) and atomic force microscopy (Digital Instruments, Nanoscope IIIa). The magnetic structures on the filaments are characterized by the magnetic force microscope (MFM). The lift scan height is set as 70 nm.

III. Results and Discussion

In most cases the electrodeposits generated by ULECD remain branching, although the branching rate has been significantly decreased[19,20] compared with the conventional scenarios. Yet there does exist a narrow window of experimental conditions where branching rate becomes extremely low, so straight filament arrays can be obtained. Normally the branching rate of the filaments decreases significantly when the separation of the filaments becomes smaller than the concentration boundary layer of growing filaments. The straight cobalt filament array is shown in Figure 2, where the periodic corrugated structures can be easily identified. The periodicity of the corrugated structure is about 100 nm. The corrugations are simultaneously generated on all filaments during the growth. As indicated inside the white circles in Figure 2, a single filament splits into two, and corrugations on the split filaments are exactly correlated.

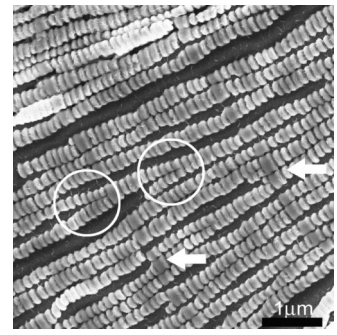

Figure 2. The scanning electron micrograph of the cobalt filament array. The white circles mark the branching regions of the filaments, where the correlation of the corrugations on adjacent filaments can be easily identified. The simultaneous generation of corrugated structures on the filaments is also illustrated by some darker bands on the filaments, which play the role of marker to trace the development of the filaments, as indicated by the white arrows.

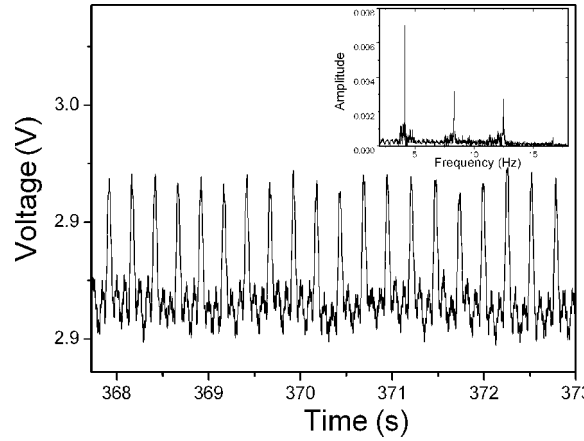

Figure 3. The electric voltage measured across the electrodes during the electrodeposition in galvanostatic mode. The inset is the Fourier transform of the voltage signal.

The simultaneous generation of the periodic corrugations on the filaments is further proven by the bands across the filaments, as indicated by the arrows in Figure 2, which are generated due to the fluctuation of chemical/physical environment in front of the growing interface in electrodeposition. The simultaneous periodic growth of the filaments is reflected on the voltage measured across the electrodes in the galvanostatic mode. As shown in Figure 3, the voltage oscillates periodically. The Fourier transform of the voltage signal indicates that the oscillation frequency is about 4.0 Hz.

The periodically corrugated structures on each filament can be tuned by changing the electric current for electrodeposition. Figure 4 shows the dependence between the periodicity on cobalt filaments and the electric current in deposition. It is clear that the spatial periodicity on the filaments decreases when the current for electrodeposition is increased.

A MFM micrograph of the filaments is shown in Figure 5. The topography of the filaments shows that the periodicity of the corrugations is about 100 nm, and the width of the filament is about 300 nm. Profile analysis indicates that the depth of the ditch between the adjacent corrugated structures on the filament is about one-third of the filament height. The distribution of the magnetic domains on filaments is shown in Figure 5b. For easier identification of the correlation of the morphology and the magnetic domains, contour of the filaments is superimposed onto the magnetic structures. One of the Co filaments has been separated slightly from the others (marked as A in Figure 5b).

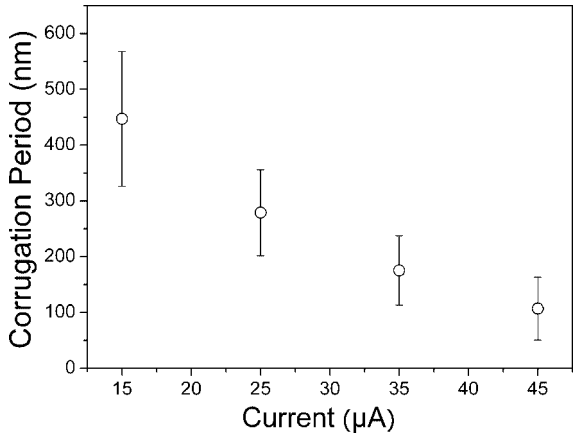

Figure 4. The plot to show the spatial periodicity on cobalt filaments measured by atomic force microscopy at different electric currents for electrodeposition.

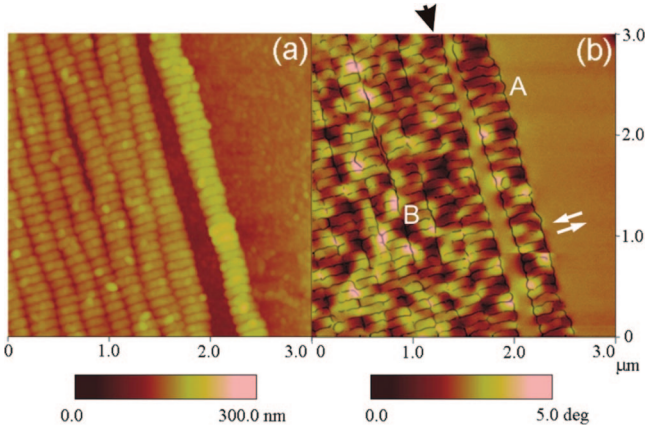

Figure 5. The MFM micrographs of the parallel cobalt filaments: (a) the topography of the filaments; (b) MFM image corresponding to the pattern shown in (a). For the convenience to compare (a) and (b), the contour of the filaments is superimposed to the MFM image.

On this separated filament, the areas with brighter and darker contrast appear alternately, forming a queue of regularly arranged domain pattern. Combining the topography and magnetic force micrograph of the filaments, we conclude that the magnetic moments are positioned antiparallel in the direction perpendicular to the filament, as illustrated by the white arrows in Figure 5b. In fact, the compromise of the gain in magnetostatic energy and the cost for domain wall formation energy leads to the antiparallel magnetic domain structures, which can also be observed in photolithography-fabricated magnetic systems.[36] In our case the domain walls locate at the ditches that separate the neighboring corrugations.

When the filaments are closely packed (the area marked as B in Figure 5b), the regularity of the magnetic domains on filaments disappears (Figure 5b). The bright regions and the dark regions are randomly positioned, except along the edge of that region (indicated by the black arrow in Figure 5b), where alternating distribution of dark and bright contrast can still be identified. We expect that the different magnetic domain conformations in regions A and B relate to the magnetic interactions between the neighboring filaments.

To confirm that the interfilament separation indeed affects the domain pattern, we fabricate a sample in which the Co filaments are straight and are separated well apart (Figure 6a). Magnetic force microscopy of the separated cobalt filaments indicates that periodically arranged domains exist on the

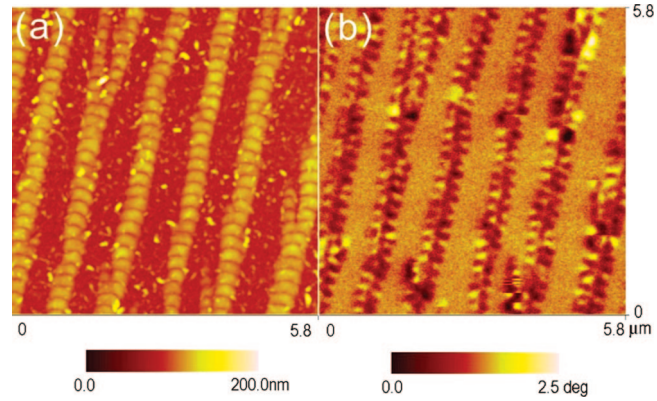

Figure 6. The MFM micrographs of the wide separated parallel cobalt filaments: (a) the topography of the filaments; (b) MFM image of the same filaments corresponding to the pattern shown in (a). Regularly arranged magnetic domains are formed on the filaments.

filament, and each domain corresponds exactly to the corrugated structure on the filament, as shown in Figure 6b.

The configuration of magnetic domains on the filaments has been simulated by a microscopic magnetic simulation software OOMMF.[37] Basically this code provides the stable magnetic states of a ferromagnetic system following an energy minimization procedure based on time integration of the Landau−Lifshitz−Gilbert equation, and magnetic dipolar interactions have been taken into account. Instead of using huge number of arrows to illustrate the local magnetization, we characterize the orientation of local magnetization with gray scale by defining the angle of local magnetic moment and x axis as θ. The contrast on each site of magnetic moment is defined as cos θ, which varies in the range of [1, −1], and is scaled to the gray scale of 0−255. For the widely separated filaments, the strongest interaction comes from the dipolar interactions within the same filament, which leads to an ordered antiferromagnetic structure, as shown in Figure 7a. When the filaments are closely packed, the interaction is much more complicated since all the surrounding magnetic units contribute to the interaction. Consequently, regular domain structure vanishes on each filament, and random domain configuration appears instead, as shown in Figure 7b. Although the detail domain patterns shown in Figure 7 are not exactly the same as those in the MFM micrographs shown in Figures 5 and 6, the essential features observed experimentally have been demonstrated in Figure 7: when the filaments are squeezed together, the magnetic domains on the filaments become random; when the filaments are well apart, the magnetic domains become much orderly arranged.

It has recently been suggested that binary information can be stored with a chain of domain walls in a ferromagnetic stripe.[17,18] By introducing a spin-polarized current pulse to the stripe, the domain walls can be simultaneously moved at the same speed over a fixed read (or write) head for sequential reading (or writing). A reverse current can move the domain walls in the opposite direction for resetting.[38] This mimics the fast passing of bits in front of the head in hard disk recording, yet the benefit is that there are no mechanical moving parts involved. Instead of using complicated microlithography techniques, our experimental observation demonstrates an easy, self-organized electrochemical way to fabricate ferromagnetic filament arrays with periodic corrugations on the surface. These corrugated structures are important to sustain the stable domain distribution. Although the experiments on electric-current-driven domain movement in our system have not been carried out yet, we expect that the fabrication method itself has already been

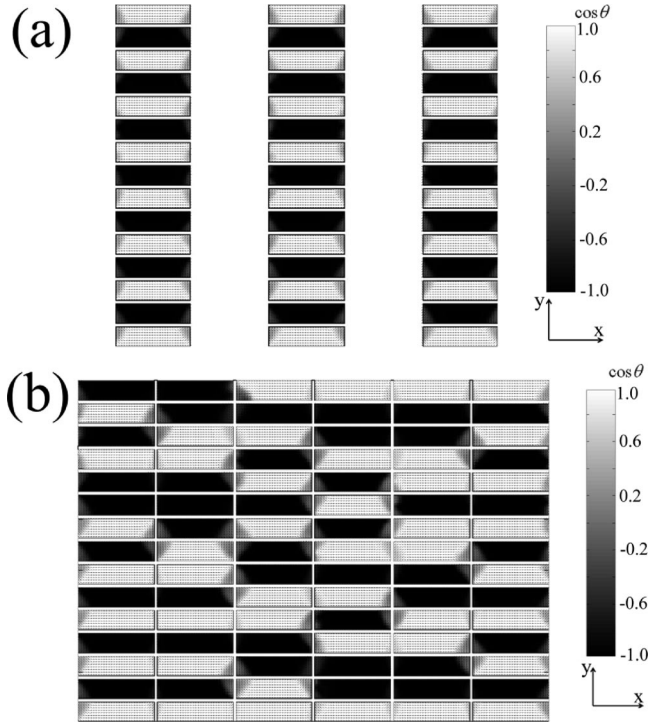

Figure 7. Micromagnetic simulations of the domain structures on the cobalt filaments. In simulation, we introduce blocks with the selected size to mimic the corrugations on the filaments. Initially on the tip of each filament, a block is added. Then the orientation of each magnetic moment therein is adjusted in order to achieve the state with minimum energy. Thereafter, new blocks are added on the very front tip of the filament, and a new turn of calculation starts. In this way, the filaments develop in $+y$ direction. (a) The regularly arranged antiferromagnetic domain structures generated when the interfilament separation is wide. (b) The situation that the filaments are closely packed, and disorder magnetic domains are formed on the filaments. The size of each block (width × length × height) is $300 \times 80 \times 40$ nm^3. The other simulation parameters are listed in ref 37.

interesting enough to attract the attention of those exploring different new materials (and structures) for data storage and magnetic logic devices.

IV. Conclusion

We show in this paper that the array of straight cobalt filaments with surface corrugations can be electrodeposited on glass substrate by ULECD without using template. The distribution of the magnetic domains on the filaments depends on the interfilament separation. Regular magnetic domains with well-aligned domain walls appear on the filaments when the interfilament separation is sufficiently wide. Once the filaments are closely positioned, disordered domain patterns are observed. These behaviors can be explained by magnetic dipolar interactions among the filaments. We suggest that this easy way of fabricating nanostructured ferromagnetic filament arrays may have potential applications in new materials for data storage and magnetic logic devices.

Acknowledgment. The work has been supported by the Ministry of Science and Technology of China (2004CB619005 and 2006CB921804) and the National Science Foundation of China (10625417 and 10874068). The authors also appreciate the discussions with H.-F. Ding and W.-W. Lin.

References and Notes

(1) Aharoni, A. *Introduction to the Theory of Ferromagnetism*; Oxford University Press: New York, 2000.
(2) Blomeier, S.; Hillebrands, B.; Reuscher, B.; Brodyanski, A.; Kopnarski, M.; Stamps, R. L. *Phys. Rev. B* **2008**, *77*, 094405.
(3) Takagaki, Y.; Ploog, K. H. *Phys. Rev. B* **2005**, *71*, 184439.
(4) Costa-Krämer, J. L.; Alvarez-Sánchez, R.; Bengoechea, A.; Torres, F.; García-Mochales, P.; Briones, F. *Phys. Rev. B* **2005**, *71*, 104420.
(5) Bolte, M.; Eiselt, R.; Meiera, G.; Kim, D. H.; Fischer, P. *J. Appl. Phys.* **2006**, *99*, 08H301.
(6) Novosad, V.; Guslienko, K. Y.; Shima, H.; Otani, Y.; Kim, S. G.; Fukamichi, K.; Kikuchi, N.; Kitakami, O.; Shimada, Y. *Phys. Rev. B* **2002**, *65*, 060402(R).
(7) Guslienko, K. Y.; Novosad, V.; Otani, Y.; Shima, H.; Fukamichi, K. *Appl. Phys. Lett.* **2001**, *78*, 3848.
(8) Shinjo, T.; Okuno, T.; Hassdorf, R.; Shigeto, K.; Ono, T. *Science* **2000**, *289*, 930.
(9) Xu, Y. B.; Hirohata, A.; Lopez-Diaz, L.; Leung, H. T.; Tselepi, M.; Gardiner, S. M.; Lee, W. Y.; Bland, J. A. C. *J. Appl. Phys.* **2000**, *87*, 7019.
(10) Novosad, V.; Grimsditch, M.; Darrouzet, J.; Pearson, J.; Bader, S. D.; Metlushko, V.; Guslienko, K. *Appl. Phys. Lett.* **2003**, *82*, 3716.
(11) Cowburn, R. P.; Koltsov, D. K.; Adeyeye, A. O.; Welland, M. E.; Tricker, D. M. *Phys. Rev. Lett.* **1999**, *83*, 1042.
(12) Verma, L. K.; Ng, V. *J. Appl. Phys.* **2008**, *103*, 053902.
(13) Ruediger, U.; Yu, J.; Zhang, S.; Kent, A. D. *Phys. Rev. Lett.* **1998**, *80*, 5639.
(14) Gao, T. R.; Yin, L. F.; Tian, C. S.; Lu, M.; Sang, H.; Zhou, S. M. *J. Magn. Magn. Mater.* **2006**, *300*, 471.
(15) Schmitte, T.; Theis-Bröhl, K.; Leiner, V.; Zabel, H.; Kirsch, S.; Carl, A. *J. Phys.: Condens. Matter* **2002**, *14*, 7525.
(16) Pan, M. H.; Liu, H.; Wang, J. Z.; Jia, J.-F.; Xue, Q.-K.; Li, J.-L.; Qin, S.; Mirsaidov, U. M.; Wang, X.-R.; Markert, J. T.; Zhang, Z.; Shih, C.-K. *Nano Lett.* **2005**, *5*, 87.
(17) Parkin, S. S. P.; Hayashi, M.; Thomas, L. *Science* **2008**, *320*, 190.
(18) Hayashi, M.; Thomas, L.; Moriya, R.; Rettner, C.; Parkin, S. S. P. *Science* **2008**, *320*, 209.
(19) Wang, M.; Zhong, S.; Yin, X. B.; Zhu, J. M.; Peng, R. W.; Wang, Y.; Zhang, K. Q.; Ming, N. B. *Phys. Rev. Lett.* **2001**, *86*, 3827.
(20) Zhong, S.; Wang, Y.; Wang, M.; Zhang, M. Z.; Yin, X. B.; Peng, R. W.; Ming, N. B. *Phys. Rev. E* **2003**, *67*, 061601.
(21) Zhong, S.; Wang, M.; Yin, X. B.; Zhu, J. M.; Peng, R. W.; Wang, Y.; Ming, N. B. *J. Phys. Soc. Jpn.* **2001**, *70*, 1452.
(22) Wang, M.; Ming, N. B. *Phys. Rev. A* **1992**, *45*, 2493.
(23) Huang, W. G.; Hibbert, D. B. *Phys. Rev. E* **1996**, *53*, 727.
(24) Lopez-Salvans, M. Q.; Sagues, F.; Claret, J.; Bassas, J. *Phys. Rev. E* **1997**, *56*, 6869.
(25) Huth, J. M.; Swinney, H. L.; Kuhn, A.; Argoul, F. *Phys. Rev. E* **1995**, *51*, 3444.
(26) de Bruyn, J. R. *Phys. Rev. Lett.* **1995**, *74*, 4843.
(27) Wang, M.; van Enckevort, W. J. P.; Ming, N. B.; Bennema, P. *Nature* **1994**, *367*, 438.
(28) Fleury, V.; Kaufman, J.; Hibbert, D. B. *Nature* **1994**, *367*, 435.
(29) Fleury, V.; Chazalviel, J. N.; Rosso, M. *Phys. Rev. Lett.* **1992**, *68*, 2492.
(30) Zhang, K. Q.; Wang, M.; Zhong, S.; Chen, G.-X.; Ming, N.-b. *Phys. Rev. E* **2000**, *61*, 5512.
(31) Matsushita, M.; Sano, M.; Hayakawa, Y.; Honjo, H.; Sawada, Y. *Phys. Rev. Lett.* **1984**, *53*, 286.
(32) Wang, M.; Ming, N.-B.; Bennema, P. *Phys. Rev. E* **1993**, *48*, 3825.
(33) Chernov, A. A. *Modern Crystallography III: Crystal Growth*, Springer-Verlag: Berlin, 1984.
(34) Ming, N. B. *Fundamental Physics of Crystal Growth*; Shanghai Science and Technology: Shanghai, 1982.
(35) Wang, Y.; Cao, Y.; Wang, M.; Zhong, S.; Zhang, M. Z.; Feng, Y.; Peng, R. W.; Hao, X. P.; Ming, N. B. *Phys. Rev. E* **2004**, *69*, 021607.
(36) Imre, A.; Csaba, G.; Ji, L.; Orlov, A.; Bernstein, G. H.; Porod, W. *Science* **2006**, *311*, 205.
(37) Detailed information can be found at http://math.nist.gov/oommf/. In our simulation, the saturation magnetization used for modeling was that of hexagonal close packed cobalt, $M_s = 1.4 \times 10^6$ A/m. The cell size was set as 10 nm, and K_1 coefficient of the magnetocrystalline anisotropy was set as zero. The exchange stiffness parameter was $A = 1.55 \times 10^{-11}$ J/m.
(38) The introductory information can be found, for example, at http://www.almaden.ibm.com/spinaps/research/sd/?racetrack.

JP807673H